Sains Malaysiana 47(2)(2018): 377-386
http://dx.doi.org/10.17576/jsm-2018-4702-20

Factors Affecting Cellulose Dissolution of Oil Palm Empty Fruit Bunch and Kenaf Pulp in NaOH/Urea Solvent

(Faktor Mempengaruhi Pelarutan Selulosa daripada Pulpa Tandan Kosong Kelapa Sawit dan Kenaf dalam Pelarut NaOH/Urea)

KHAIRUNNISA WAZNAH BAHARIN, SARANI ZAKARIA*, AMANDA V. ELLIS, NORAINI TALIP, HATIKA KACO, SINYEE GAN, FARRAH DIYANA ZAILAN & SHARIFAH NURUL AIN SYED HASHIM

ABSTRACT

The factors responsible for the low solubility percentage of oil palm empty fruit bunch (OPEFB) cellulose pulp compared to kenaf when dissolved in aqueous NaOH/urea solvent system was reported. Physical and chemical properties of both cellulose pulp were studied and compared in terms of the lignin content, viscosity average molecular weight (Mη), crystallinity index (CrI), cellulose pulp structure and their zero span tensile strength. The structure of both OPEFB and kenaf cellulose pulp were characterized using high powered microscope and field emission scanning electron microscopy (FESEM) assisted by ImageJ® software. The results show that the most significant factor that affected the OPEFB and kenaf cellulose dissolution in NaOH/-urea solvent was the Mη with OPEFB having a higher Mη of 1.68×10^5 compared to 5.53×10^4 for kenaf. Overall, kenaf cellulose appeared to be produced in higher quantities presumably due to its lower molecular weight with superior tensile strength and permeability in comparison to OPEFB.

Keywords: Cell wall thickness; lumen size; solubility percentage; XRD

ABSTRAK

Faktor menyebabkan peratus pelarutan selulosa tandan kosong kelapa sawit (TKKS) yang rendah berbanding selulosa kenaf apabila dilarutkan di dalam sistem pelarut akueus NaOH/urea dilaporkan. Sifat fizikal dan kimia selulosa dari pulpa TKKS dan kenaf dikaji dan dibandingkan dari segi kandungan lignin, purata berat molekul (Mη), indeks penghabluran (CrI), struktur pulpa selulosa dan kekuatan tegangan zero-span. Struktur kedua-dua pulpa selulosa dilihat dan dikaji dengan menggunakan mikroskop berkuasa tinggi dan (FESEM) dibantu dengan perisian ImageJ®. Daripada pencirian yang telah dijalankan, faktor yang memberikan kesan paling signifikan kepada pelarutan selulosa adalah berat molekul pulpa memandangkan berat molekul pulpa OPEFB yang diperolehi adalah lebih tinggi daripada kenaf dengan 1.68×10^5 dan 5.53×10^4 masing-masing. Secara keseluruhannya, dianggarkan kandungan selulosa daripada kenaf adalah lebih tinggi disebabkan berat molekul yang rendah tetapi mempunyai kekuatan tegangan dan kebolehtelapan yang lebih baik daripada TKKS.

Kata kunci: Ketebalan dinding sel; peratus keterlarutan; saiz lumen; XRD

INTRODUCTION

Cellulose is one of the most abundant polysaccharides on earth and a significant natural resource, with approximately 1.5×10^{12} tonnes produced annually worldwide (Liu et al. 2013; Wang & Deng 2009). Cellulose was first identified by a distinguished French scientist, Anselme Payen in 1838 during the treatment of different wood and plant tissue with nitric acid. Payen then introduced and named the stable fibrous substance obtained from the treatment as cellulose in 1839 (Eichhorn et al. 2001; Rowell & Young 1978). Cellulose is made up of repeating units of anhydroglucopyranose rings ($(C_6H_{10}O_5)_n$) linked together by an oxygen covalently bonded to the C1 of one glucose ring and the C4 of the adjoining ring (1→4 linkage), the so called β 1-4 glycosidic bond (Moon et al. 2011). Although cellulose is predominantly obtained from plants, it can also be found in animal kingdom, specifically in tunicin, the cuticular substance of tunicates (marine invertebrate animals) (Zhou & Li 2014).

Recent progress in the modification of cellulose to produce stable cellulose derivatives has gained and renewed interest in this area (Kaco et al. 2014). In particular it has now been shown that the properties of cellulose can be enhanced through chemical or physical modification and also by the addition of functional fillers (Gan et al. 2014; Li et al. 2012). For instance, to this date cellulose derivatives has been used for coating, lamination, film optics, cellophane, rayon, cellulose acetate and as absorption media (Gan et al. 2014; Li et al. 2012).

The total global annual yield of OPEFB is over 45 million tons (Nurdiawati et al. 2015). In Malaysia, oil palm trees have become one of the main agricultural plants which has contributed to an increase in economic growth for the country (Lamaming et al. 2015) besides

helped in the removal of large amount of CO_2 from the atmosphere as has been reported in recent studies (Kho & Jepsen 2015). The oil palm cellulose can be utilized as composite board, biodiesel, organic fertilizer and paper (Law et al. 2007). OPEFB also come from a non-woody plant with a composition of 48 to 65% cellulose, 15 to 25% hemicellulose and 20 to 24% lignin (Nazir et al. 2013). To date, the physical and chemical nature of OPEFB cellulose has not been fully investigated and thus it is important to gather more information on OPEFB in order to utilize it to the fullest.

While kenaf is a Hibiscus (*Hibiscus cannabinus* L.), which is a part of the Malvaceae (Mallow) family (Gan et al. 2014). Kenaf can grow over 3 m in 3 months making it the fourth most favourable industrial crops in Malaysia (Sajab et al. 2011). Its fiber provides vast amount of biomass which are economically cheaper to produce than other natural fibers produced in Malaysia (Saba et al. 2016). Kenaf core fiber consists of around 46.1% cellulose, 29.7% hemicellulose and 22.1% lignin (Ching & Ng 2014; Gan et al. 2014).

In general, the major problem with cellulose is its insolubility which is attributed to the intricate network of intra and inter- molecular hydrogen bonds, making cellulose difficult to be dissolved in comon solvent (Alves et al. 2015). Examples of solvents for non-derivitised cellulose are cuaxam, cadmium ethylenediamine (cadoxen), cuen, N, N-dimethylacetamide (DMAc/LiCl), dimethylsulfoxide (DMSO) and triethylamine. Meanwhile, the examples of solvents for derivitised cellulose are *N, N*–dimethylformamide and dinitrogen tetroxide (DMF/N_2O_4), formic acid (HCOOH) and trifluoroacetic acid (CF_3COOH) (Cai & Zhang 2005; Luo & Zhang 2013). However, many of the alkali metallic complex solvents involve oxidation processes which are unstable, toxic, coloured and may degrade the properties of cellulose aside from jeopardizing the environment (Zhou et al. 2004).

NaOH/urea solvent systems have been widely used on plants such as cotton linter, kenaf and bagasse (Zhou & Zhang 2000). This alkaline urea solvent system is popular due to its low cost and speed of cellulose dissolution (Gan et al. 2015b). The main factors that affect cellulose dissolution can be classified into: external factors - such as the type of solvent used and the pulping process and internal factors - such as the physical and chemical properties of the fiber itself. Siqueira et al. (2010) have proposed that if the solvent system (internal factor) is kept constant than the cellulose dissolution rates may differ due to the degree of polymerization, molecular weight, crystallinity and the structure of fiber itself, which varies according to plant species.

Therefore, this work aimed to determine the difference between OPEFB and kenaf cellulose when dissolved via the pre-cooled dissolution process in aqueous NaOH/urea solvent.

Materials and Methods

Materials

The OPEFB pulp sheet was obtained from Eko Pulp & Paper Sdn. Bhd and the kenaf core pulp was obtained from Malaysian Agricultural Research and Development Institute (MARDI). Sodium chlorite ($NaClO_2$), acetic acid, sodium hydroxide (NaOH), urea, sulphuric acid (H_2SO_4) ethylene diamine ($C_2H_4(NH_2)_2$) and cadmium oxide (CdO) used in this study were purchased from Sigma Aldrich and used as received.

Chlorite Bleaching and Alkaline Treatment

The work flow of this treatment is illustrated as in Figure 1. The oven dried disintegrated pulp (35 g) was bleached through D-E-E-D treatment series where D and

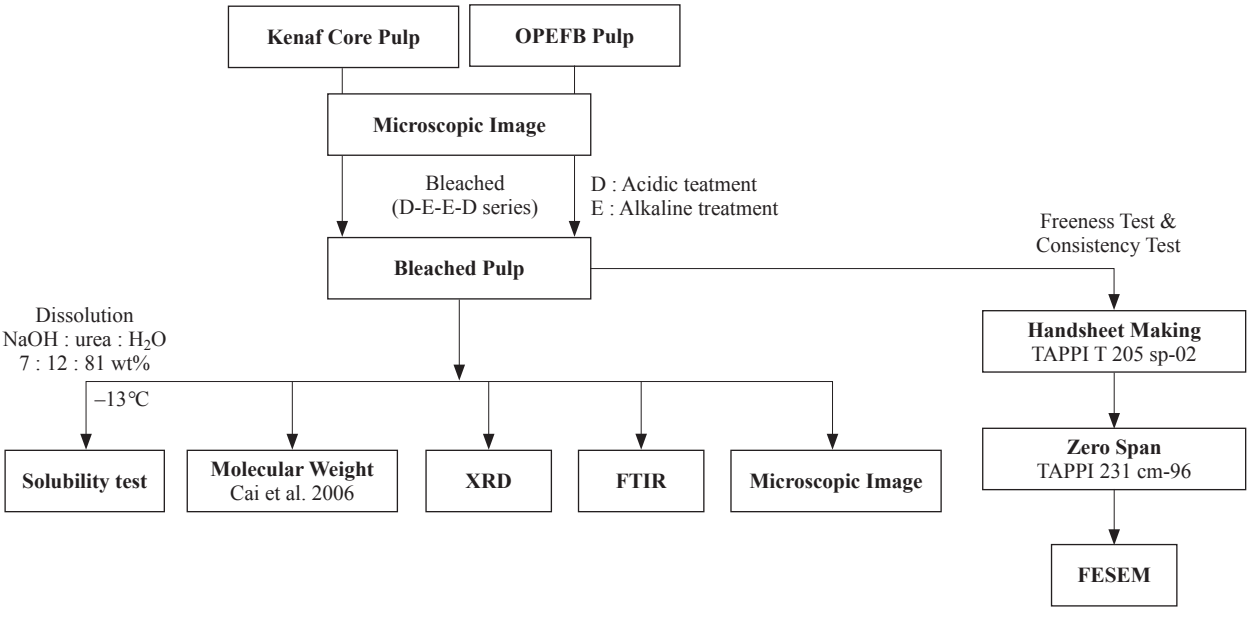

FIGURE 1. Design illustration of method and analysis used

E involved chemical treatment of 1.7% sodium chlorite (delignification) and 4% to 6% sodium hydroxide (alkaline treatment), respectively. The mixture was treated at 80°C in water bath at each stage and washed with distilled water until neutral afterward to remove any excessive bleaching chemicals before entering the next stage. Lignin and hemicellulose was removed to obtain the bleached pulp of OPEFB and kenaf cellulose. After the D-E-E-D treatment series, the pulp was dried at 105°C in an oven for 24 h.

LIGNIN CONTENT

The lignin content of the OPEFB and kenaf pulp were determined according to the TAPPI standard T222 om-06 (T222) (standard by Technical Association of the Pulp and Paper Industry) which refers to Acid Insoluble Lignin in Wood and Pulp. Both samples were hydrolyzed with 72% sulfuric acid at 20°C for 2 h and then solubilized at 100°C for 4 h. The acid insoluble lignin was filtered and the residue was dried at 105°C overnight before being weighed. The percentage of lignin content was then calculated according to (1).

$$\text{Lignin (\%): } A = \left[\frac{100}{W}\right] \tag{1}$$

where A is the weight of lignin in g and W is the dry weight of sample in g (which is 1 g).

VISCOSITY AVERAGE MOLECULAR WEIGHT (MH)

The viscosity average molecular weight ($M\eta$) is one of the physical properties that can be obtained from the pulp and fiber characterisation. Cellulose pulp from both OPEFB and kenaf were dissolved in cadoxen solution and measured at 25°C using an Ubbelohde capillary viscometer to obtain the intrinsic viscosity [η] of the solution. Both cellulose pulps were dissolved in cadoxen solution at concentration of 3×10^3 g/mL and diluted for 5 times to achieve a concentration ranging from 1.0×10^{-5} to 4×10^{-3} g/mL. The intrinsic viscosities of the samples were determined by extrapolation to zero concentration of the Huggins and Kraemer equations shown in (2) and (3), respectively. A plot of the inherent viscosity, extrapolated to zero concentration, yields the intrinsic viscosity (Cai et al. 2006; Kaco et al. 2014).

The Huggins equation is derived from a virial expansion expression of the specific viscosity in powers of the intrinsic viscosity whereas the Kraemer equation results from an expansion of the inherent viscosity to determine the intrinsic viscosity.

$$\frac{\eta_{sp}}{C} = [\eta]C = k_H[\eta]^2C. \tag{2}$$

$$\frac{\ln(\eta_r)}{C} = [\eta]C = k_H[\eta]^2C. \tag{3}$$

The constant k_H and k_K are termed as the Huggins and Kraemer coefficient, respectively, and C is the cellulose concentration. By inserting the intrinsic viscosity into (4) and (5), the degree of polymerization (DP) and the M_η can be calculated.

$$DP = \left[\frac{[\eta]}{1.75}\right]^{\left[\frac{1}{0.69}\right]}. \tag{4}$$

$$M_\eta = \left[\frac{[\eta]}{3.85 \times 10^{-2}}\right]^{\left[\frac{1}{0.76}\right]}. \tag{5}$$

X- RAY DIFFRACTOMETRY (XRD)

XRD was used to analyze the crystallinity of cellulose as well as to determine the arrangement of atoms and crystallite size. Samples of cellulose pulp (0.05 g) from both OPEFB and kenaf were tested. D8 Advance Bruker AXS with DIFFRAC TOPAS software (Germany) was employed using a radiation of $Cu\ K\alpha = 1.5458$ Å at diffraction angle of 2θ ranging from 5° to 80°. The operating power was 40 kV and 40 mA. The percentage crystallinity of both samples were obtained by using the Segal equation (6) where $A_{Crystal}$ is the area under the crystalline diffraction peaks and A_{Total} is the total area under the diffraction curve between 2θ = 5° and 80°.

$$CrI(\%) = A_{Crystal}/A_{Total} \times 100 \tag{6}$$

ATTENUATED TOTAL REFLECTANCE-FOURIER TRANSFORMED INFRARED SPECTROSCOPY (ATR-FTIR)

The fibers were analyzed using Attenuated Total Reflectance-Fourier Transformed Infrared Spectroscopy (ATR-FTIR), Bruker Alpha equipped with OPUS software measured at wavenumber within the range of 4000-800 cm^{-1}.

HANDSHEET MAKING

The handsheet of OPEFB and kenaf pulp were produced at the Forest Research Institute Malaysia (FRIM). The following briefly describes their production which followed the standard by Technical Association of the Pulp and Paper Industry *(TAPPI T205 sp-02)*. The cellulose pulp (30 g) were added into 2000 mL distilled water at 20 ± 2°C and disintegrated at 3000 rpm to disperse all fiber bundle. The stock solution then was added and dispersed in 7.0 L of distilled water before being poured into the cylinder of the handsheet maker. The hand sheets were formed by rapid movement of water through the sheet drained under suction. After pressing, the hand sheets were dried at ambient temperature using drying ring. The freeness of pulp Canadian standard method (T227 om-99) was also carried out to measure the rate of pulp drainage.

ZERO-SPAN TENSILE STRENGTH

This test measures the tensile strength at the moment of tensile failure of pulp randomly oriented in a sheet form. In this test method, the pulps were tested as a handsheet produced using a standardized procedure such as TAPPI T205. The zero-span tensile data is important to determine the maximum strength of pulp fibers having a grip separation of 0.00 mm (0.000 in) according to TAPPI 231 cm-96, standard by Technical Association of the Pulp and Paper Industry. Each test sheet was cut into strips of a

size suit to the zero-span tensile jaw and to a width which exceeded the width of the clamping jaw. The clamping width and clamping length was not less than 15.0 and 0.60 mm, respectively. At least 10 replicates were made for each sample to determine the average zero-span value.

The zero-span tensile test value of OPEFB and kenaf samples was calculated using (7).

$$\text{Zero-span value, N/cm} = \frac{\textit{Measured value}\,(N)\left(\dfrac{60}{\textit{Strip grammage}}\right)}{\textit{Jaw width}\,(cm)} \quad (7).$$

FESEM

The cross section of the pulp were studied using a field scanning electron microscope (FESEM) ZEISS Merlin Compact. The samples which were in hand sheet form was immersed in liquid nitrogen and subsequently freeze dried for 24 h. Afterwards, the freeze dried samples were torn horizontally and sputter coated with platinum before analysed.

IMAGEJ® SOFTWARE

ImageJ® is an image processing and analysis software in Java where the selected area or line are created by using freehand line selection tools. The lumen size and the pulp diameters were analysed and measured according to the image obtained from FESEM which was calibrated with the software before-hand (Chinga-Carrasco et al. 2013; Hartig 2013).

SOLUBILITY OF OPEFB AND KENAF BLEACHED PULP IN AQUEOUS NAOH-UREA SOLVENT SYSTEM

OPEFB and kenaf cellulose pulp (3 g) were dissolved in total volume of 50 mL NaOH/urea solvent with the optimized weight ratio of 7 wt. % NaOH, 12 wt. % urea and 81 wt. % H_2O solvent via rapid dissolution method as reported by previous studies (Kaco et al. 2014; Zhang et al. 2010). The composition of NaOH/urea was fixed so that the differences in the solubility percentage of both OPEFB and kenaf cellulose can be directly compared. NaOH/urea solvent was pre-cooled in freezer for at least 6 h prior to use and cellulose was added when the temperature of the solvent reached –12.8°C. The mixture was stirred using a mechanical stirrer at 1200 rpm to get a homogenous solution and centrifuged at 10000 rpm for 5 min to separate the dissolved and undissolved parts. The undissolved cellulose was usually in the form of a gel-like precipitate at the bottom part of the centrifuge tube. This was washed with excess distilled water until the pH was neutral and then dried at 105°C overnight before being weighed. Both dissolution and solubility tests were repeated at least three times. The solubility, S_a, was then calculated from (8).

$$S_a = \left[\frac{W_1 - W_2}{W_1}\right] \times 100\%. \quad (8)$$

where W_1 is the weight of original cellulose and W_2 is the weight of undissolved cellulose.

RESULTS AND DISCUSSION

LIGNIN CONTENT

Chlorite bleaching and alkaline treatment is designed to remove lignin, hemicellulose and other impurities in order to obtain pure cellulose which also leading to the defibrillation of cellulose. Defibrillated cellulose will enhance the dissolution as more solvent could penetrate into cellulose as the total surface area increases (Gan et al. 2015a; Siqueira et al. 2010). Therefore, the lignin content for OPEFB pulp sheet and kenaf after the D-E-E-D bleaching series had reduced up to 88% and 95%, respectively. The result indicated that both cellulose pulp has removed most of the lignin through the bleaching treatment due to the cleavage of ether linkages between lignin and hemicellulose (Chirayil et al. 2014; Xiao et al. 2001). However, the difference in the lignin content between the bleached OPEFB and kenaf cellulose is small.

VISCOSITY AVERAGE MOLECULAR WEIGHT (Mη)

The chemical structure in all wood based cellulose is almost the same, therefore the same characterisation can be used. One factor to consider in cellulose chemical structure is the length of the cellulose chains which is related to the degree of polymerisation (DP) and its variation in different plant species (Siqueira et al. 2010). The variation of DP and molecular weight distribution are one of the major factors influencing the properties of a polymer such as its crystallinity and solubility (Olson & Westman 2013). Figure 2 shows the plot of the specific viscosity and relative viscosity (Huggins-Kraemer equation) against cellulose concentration for the OPEFB and kenaf cellulose pulps which were dissolved in cadoxen solution at 25°C (Kaco et al. 2014). From Table 1 it can be seen that the OPEFB cellulose has higher $M\eta$ compared to kenaf as well as the degree of DP of both cellulose is directly proportional to their $M\eta$ with 2255 for OPEFB and 664 for kenaf.

X-RAY DIFFRACTION SPECTROMETER (XRD)

Figure 3(a) and 3(b) shows the XRD patterns of OPEFB and kenaf cellulose pulps before and after bleaching treatment. Both samples showed the diffraction peaks at $2\theta = 14.9°$, 16.3°, 22.6° and 34.5° which can be assigned to cellulose I crystal planes of (1 $\bar{1}$ 0), (1 1 0), (2 0 0) and (0 0 4), respectively (Ching & Ng 2014; Nazir et al. 2013). Cellulose contains both crystalline and amorphous regions and the latter is reported to be more easier to dissolve due to more accessible region of the solvent thus facilitate the dissolution (Alves et al. 2015). The removal of lignin and hemicelluloses, both in amorphous regions, has increased the crystallinity index (CrI) crystallinity of cellulose after bleaching process for both OPEFB and kenaf cellulose with 0.1% and 1.6%, respectively. The lignin content result also indicates that the lignin removal in kenaf is slightly higher compared to OPEFB.

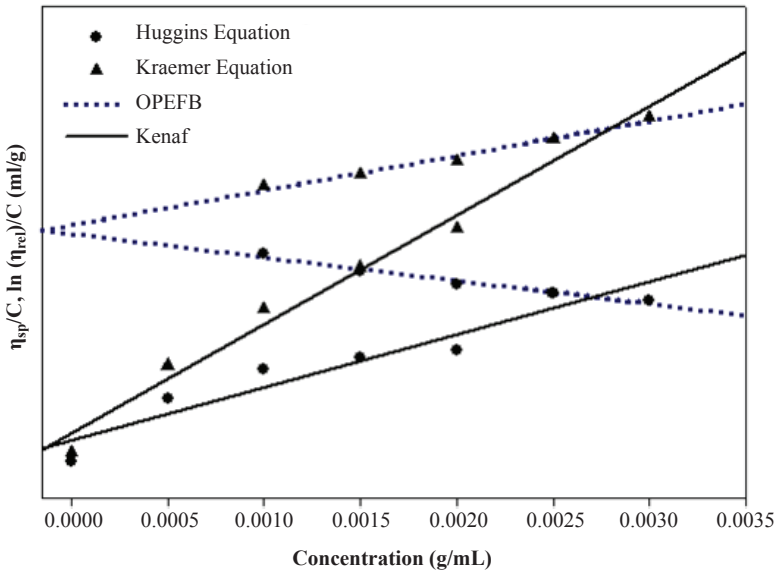

FIGURE 2. Huggins-Kraemer equation against concentration of OPEFB and kenaf cellulose at 25°C of cadoxen solution

TABLE 1. Experimental result of average viscosity and molecular weight of OPEFB and kenaf fibre

Sample	Concentration 1×10^{-3} (g/mL)	Relative viscosity ln η_{rel}/c (1×10^2)	Specific viscosity η_{sp}/c (1×10^2)	Average molecular weight
Bleached OPEFB	3.0	3.48	4.87	
	2.5	3.31	4.64	
	2.0	3.17	4.42	1.68×10^5
	1.5	3.08	4.28	
	1.0	3.00	4.17	
Bleached Kenaf	3.0	2.51	3.74	
	2.5	2.43	3.35	
	2.0	2.30	2.93	5.53×10^4
	1.5	2.01	2.35	
	1.0	1.37	1.47	

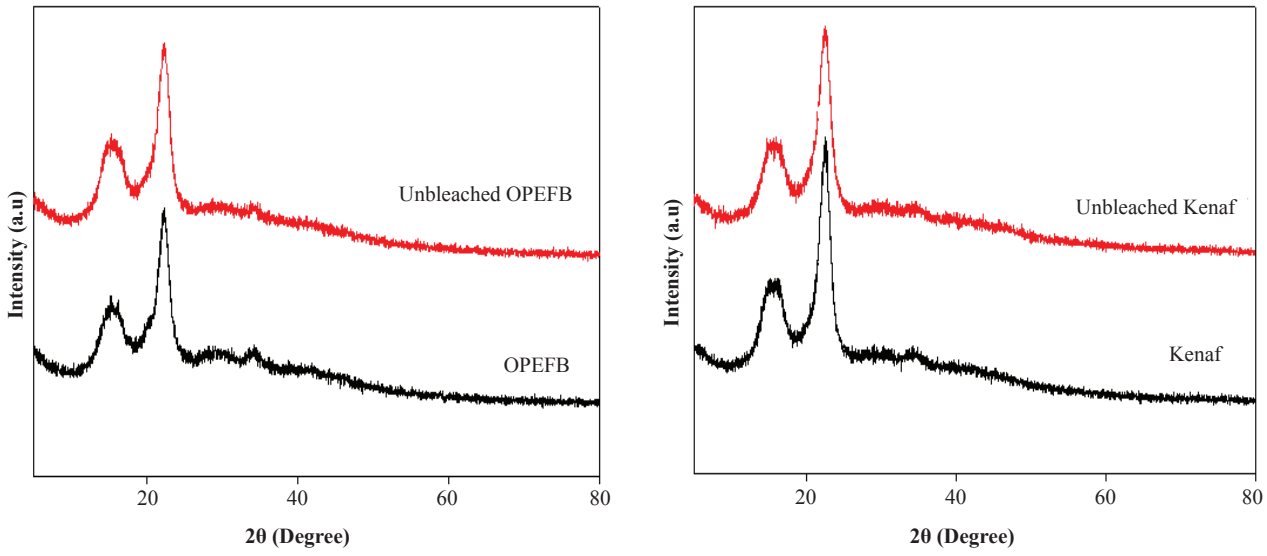

FIGURE 3. Wide-angle X-ray diffraction (XRD) analysis of bleached (a) OPEFB and (b) kenaf cellulose before and after bleaching

ATR-FTIR

As presented in Figure 4(a) and 4(b), both OPEFB and kenaf cellulose pulp showed the similarity of the ATR-FTIR spectra indicating the similar chemical compositions but slight difference can be seen between bleached and unbleached pulp. According to previous studies, the most characteristic infrared bands of lignin can be found at about 1510 and 1600 cm^{-1} (aromatic ring vibrations) and between 1470 and 1460 cm^{-1} (C-H deformations and aromatic rings vibration). The first mentioned wavenumber region is poor in additional bands and can therefore be used to prove the existence of lignin prepared at any condition (Fengel & Wegener 1989). These peaks are shown to disappear after the bleaching process due to the effects of the alkali and chlorite bleaching treatment (Ching & Ng 2014). The peaks between 1330 and 1370 cm^{-1} correspond to the units of $–CH_2$ and C-H of cellulose, respectively. Two peaks at approximately 1210 and 1640 cm^{-1} represent the bending vibrations of the OH groups of cellulose (Gan et al. 2015b). The broadened band of the OH stretching oscillation (3200-3300 cm^{-1}) is an indication of a high portion of water linked to cellulose-OH.

ZERO-SPAN TENSILE STRENGTH

Zero-span breaking strength is a quick and reliable method to measure the zero-span tensile strength of a randomly oriented specimen of fibers when dry. Table 3 shows that kenaf has a higher fiber strength at 4.6 N/m

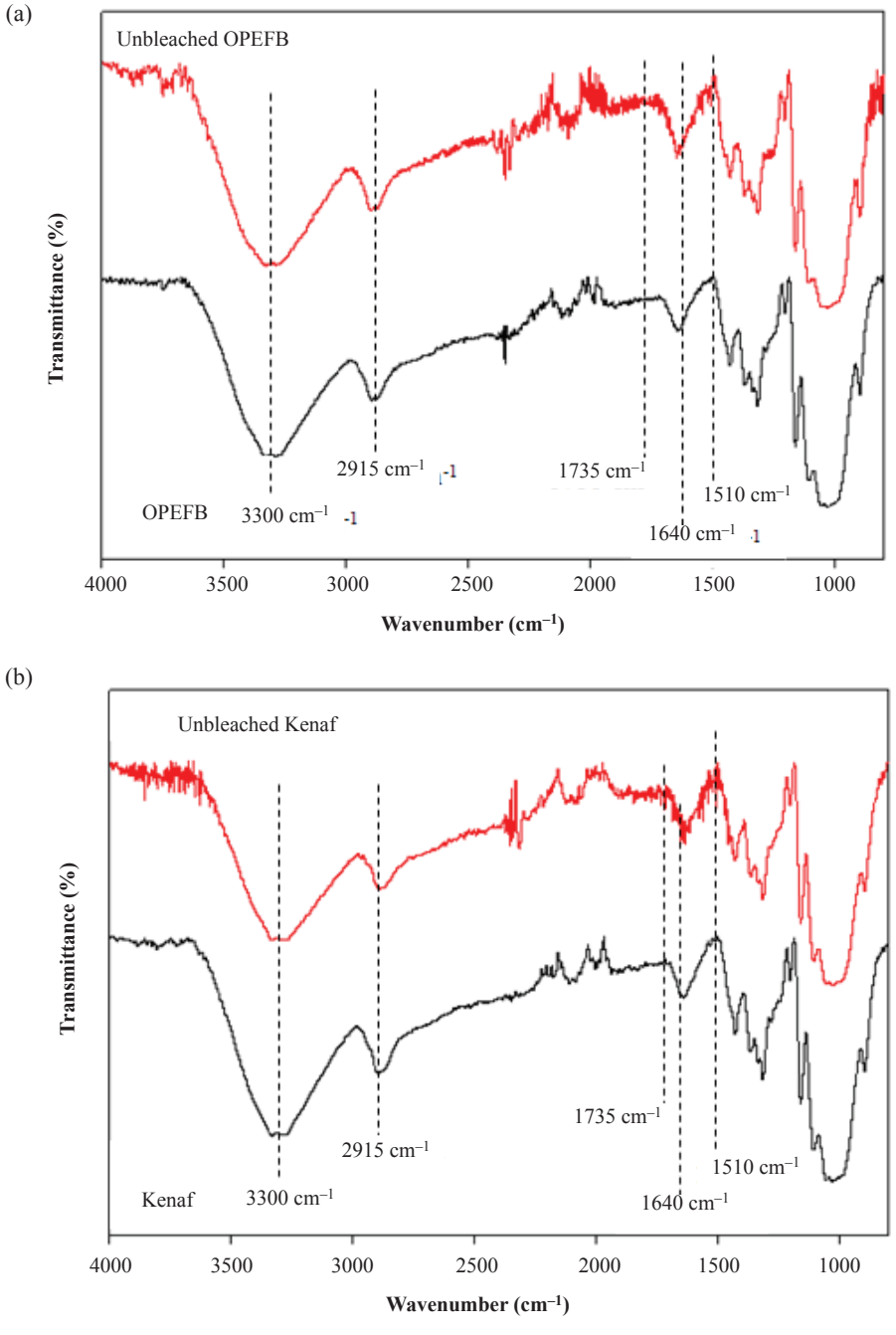

FIGURE 4. ATR-FTIR spectra of (a) OPEFB and (b) kenaf cellulose before and after bleaching

compared to 1.7 N/m for OPEFB. One of the factors that could affect the tensile strength is the crystallinity where higher crystallinity indicates a solid cellulose arrangement thus enhanced the tensile strength (Chirayil et al. 2014). Meanwhile, the freeness test which measure how quickly dilute suspension of pulp may be drained shows that kenaf has higher freeness compared to OPEFB. According to Pulp & Paper Resource & Information Site in 2017, the freeness result might be affected by the pulp length as long pulp gives higher freeness whereas short pulp or fines will reduced the pulp freeness.

IMAGE ANALYSIS USING IMAGEJ® SOFTWARE (FESEM & MICROSCOPIC IMAGE)

Table 2 shows the range of average lumen sizes or the lumen perimeter and diameters of the fibers measured using ImageJ software from the optical microscope and FESEM images. The image of unbleached and bleached OPEFB and kenaf cellulose are presented in Figure 5. The result illustrate that after bleaching process, the kenaf cellulose become collapsed and less dense compared to OPEFB cellulose which seemed to remains its structure even after the bleaching treatment. Whilst Figure 6 is the FESEM images of OPEFB and kenaf cellulose from top view which illustrate that kenaf has thicker cell wall compared to OPEFB indicating the presence of more cellulose with low average viscosity molecular weight. Even though less cellulose can be seen in OPEFB, the molecular weight of the cellulose were high (Strunk 2012). This might be one of the reason for the result of higher solubility of kenaf cellulose as the cellulose content is much higher than in OPEFB even when prepared at the same dry weight of cellulose.

SOLUBILITY OF OPEFB AND KENAF BLEACHED PULP IN AQUEOUS NAOH/UREA SOLVENT SYSTEM

The solubility, S_a of OPEFB and kenaf pulp in 50 mL NaOH/urea solvent obtained was 40% and 93%, respectively. The mechanism of cellulose dissolution in NaOH/urea solvent was activated by the formation of inclusion complex (IC) around the cellulose or often terms as 'swelling' as the NaOH molecule break the inter- and intra

TABLE 2. Average lumen size and cell wall of OPEFB and kenaf fibre

Pulp	(FESEM) image		Optical microscope image
	Average lumen perimeter (μm)	Average cell wall (μm)	Average diameter (μm)
OPEFB	15.32-16.89	1.56-2.57	18.56
Kenaf	15.12-15.83	2.56-3.45	23.06

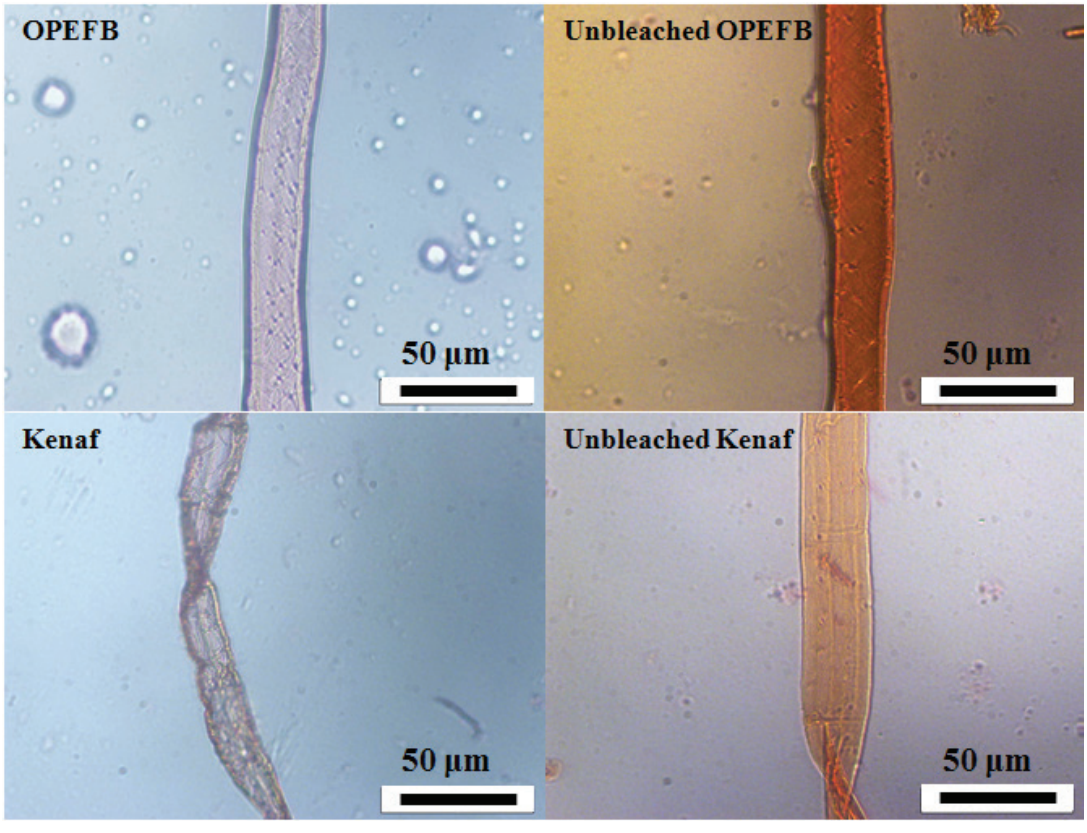

FIGURE 5. Optical microsope images of OPEFB and kenaf cellulose before and after bleached

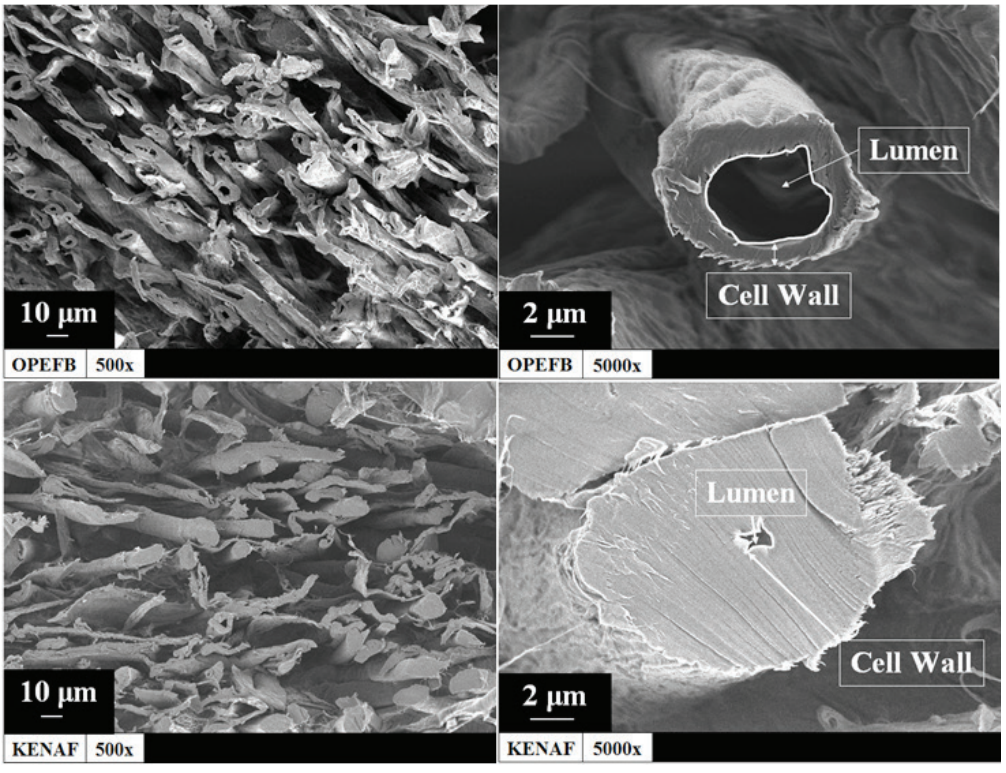

FIGURE 6. Cross section of OPEFB and kenaf cellulose under FESEM

TABLE 3. Zero-span tensile strength of OPEFB and kenaf fibre

Pulp	Mean (N/cm)	Standard deviation
OPEFB	1.76	0.13
Kenaf	4.76	0.18

TABLE 4. Freeness test of OPEFB and kenaf fibre

Pulp	Mean (mL/s)	Standard deviation
OPEFB	537	72.1
Kenaf	749.5	9.2

molecular hydrogen bond between cellulose while urea hydrate preventing the aggregation of cellulose (Kaco et al. 2014; Zhou & Zhang 2000). Centrifugation used to separate the solution into undissolved and dissolved cellulose was indicate by the two distinct phase formed in the cellulose solution (Figure 7). The undissolved phase of OPEFB cellulose consisted of a thick gel-like solution at the bottom part of the centrifuge tube and a low viscosity dissolved cellulose supernatant solution. Meanwhile, the kenaf cellulose solution, after centrifugation, showed only a small amount of undissolved cellulose and a very viscous supernatant cellulose solution. The viscous supernatant can be further used to fabricate good regenerated cellulose products.

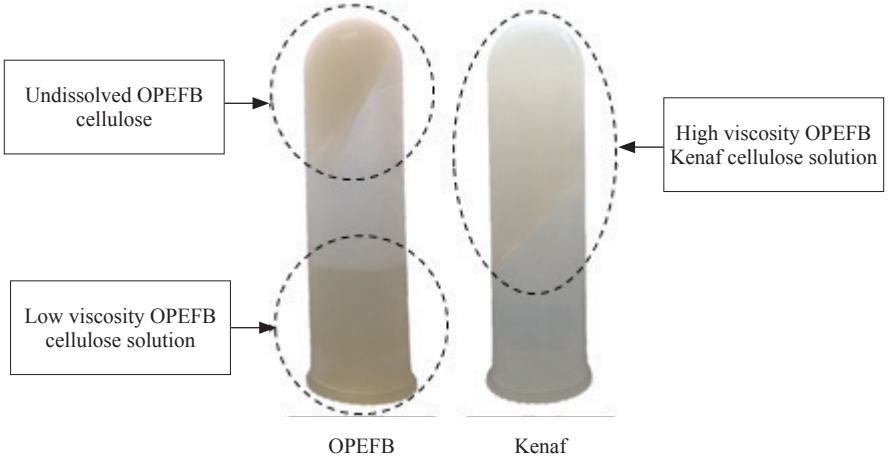

FIGURE 7. The OPEFB and kenaf cellulose solution after centrifugation

The low solubility of OPEFB can be attributed by the high molecular weight and degree of polymerization as this could affect the penetration of NaOH and alkaline urea solvent into OPEFB compared to kenaf. The slightly higher lignin content, rigid pulp structure, less cellulose in single pulp, low crystallinity and also low freeness are the additional factor that leading to the low degree of dissolution.

CONCLUSION

OPEFB shows a higher molecular weight than kenaf at 1.68×10^5 and 5.53×10^4, respectively, making its solubility in NaOH/urea solvent less effective than kenaf. The OPEFB cellulose also have thinner cell walls, a rigid structure yet low crystallinity index and higher lignin content compared to kenaf. Meanwhile, kenaf cellulose fibre surpasses OPEFB in strength at 4.6 N/m compared to 1.7 N/m for OPEFB and has higher cellulose permeability. As kenaf cellulose appears to be produced in higher quantities presumably due to its lower molecular weight with superior properties in comparison to OPEFB, this product shows great potential as a high-end product for industrial applications. However, additional treatment can be done on OPEFB fibre to reduce its molecular weight thus enhancing its cellulose dissolution.

ACKNOWLEDGEMENTS

The authors would like to thank Universiti Kebangsaan Malaysia and Forest Research Institute Malaysia (FRIM) for providing laboratory facilities and financial assistance under project code MRUN-2015-003 and LRGS/TD/2012/USM-UKM/PT/04. The authors would also like to express our special gratitude to UKM Microtechnique and Plant Anatomy Research Team for knowledge-sharing and providing plant anatomy research facilities.

REFERENCES

Alves, L., Medronho, B., Antunes, F.E., Topgaard, D. & Lindman, B. 2015. Dissolution state of cellulose in aqueous systems. 1. Alkaline solvents. *Cellulose.* DOI 10.1007/s10570-015-0809-6.

Cai, J. & Zhang, L. 2005. Rapid dissolution of cellulose in LiOH/urea and NaOH/urea aqueous solutions. *Macromolecular* 41: 9345-9351.

Cai, J., Liu, Y. & Zhang, L. 2006. Dilute solution properties of cellulose in LiOH/urea aqueous system. *Journal of Polymer Science Part B: Polymer Physics* 44(21): 3093-3101.

Ching, Y.C. & Ng, T.S. 2014. Effect of preparation conditions on cellulose from oil palm empty fruit bunch fiber. *BioResources* 9(4): 6373-6385.

Chinga-Carrasco, G., Solheim, O., Lenes, M. & Larsen, A. 2013. A method for estimating the fibre length in fibre-PLA composites. *Journal of Microscopy* 250: 15-20.

Chirayil, C.J., Joy, J., Mathew, L., Mozetic, M., Koetz, J. & Thomas, S. 2014. Isolation and characterization of cellulose nanofibrils from *Helicteres* isora plant. *Industrial Crops and Products* 59: 27-34.

Eichhorn, S.J., Baillie, C.A., Mwaikambo, L.Y., Ansell, M.P., Dufresne, A., Entwistle, K.M., Herrera, P.J., Escamilla, G.C., Groom, L., Hughes, M., Hill, C., Rials, T.G. & Wild, P.M. 2001. Current international research into cellulosic fibers and composites. *Journal of Materials Science* 36: 2107-2131.

Fengel, D. & Wegener, G. 1989. *Wood: Chemistry, Ultrastructure, Reactions*. Location: Walter de Gruyter & Co., Berlin. pp. 1-174.

Gan, S.Y., Zakaria, S., Chia, C.H., Padzil, F.N.M. & Ng, P. 2015a. Effect of hydrothermal pretreatment on solubility and formation of kenaf cellulose membrane and hydrogel. *Carbohydrate Polymers* 115: 62-68.

Gan, S.Y., Padzil, F.N.M., Zakaria, S., Chia, C.H., Syed Jaafar, S.N. & Chen, R.S. 2015b. Synthesis of liquid hot water cotton linter to prepare cellulose membrane using NaOH/urea or LiOH/urea. *BioResources* 10(2): 2244-2255.

Gan, S.Y., Zakaria, S., Chia, C.H., Kaco, H. & Padzil, F.N.M. 2014. Synthesis of kenaf cellulose carbamate using microwave irradiation for preparation of cellulose membrane. *Carbohydrate Polymers* 106: 160-165.

Pulp & Paper Resource & Information Site. 2017. Properties of pulp. http://www.paperonweb.com/pulppro.html. Accessed on 15 July 2017.

Hartig, S.M. 2013. Basic image analysis and manipulation in image j. *Current Protocols in Molecular Biology* 102: 14.15.1-14.15.12.

Kaco, H., Zakaria, S., Razali, N.F., Chia, C.H., Zhang, L. & Jani, S.M. 2014. Properties of cellulose hydrogel from kenaf core prepared via pre-cooled dissolving method. *Sains Malaysiana* 43(8): 1221-1229.

Kho, L.K. & Jepsen, M.R. 2015. Carbon stock of oil palm plantations and tropical forests in Malaysia: A review. *Singapore Journal of Tropical Geography* 36: 249-266.

Lamaming, J., Hashim, R., Leh, C.P., Sulaiman, O., Sugimoto, T. & Nasir, M. 2015. Isolation and characterization of cellulose nanocrystals from parenchyma and vascular bundle of oil palm trunk (*Elaeis guineensis*). *Carbohydrate Polymer* 10(134): 534-540.

Law, K.N., Wan Daud, W.R. & Ghazali, A. 2007. Morphological and chemical nature of fiber strands of oil palm empty fruit bunch (OPEFB). *BioResources* 2: 351-362.

Li, Q., Wu, P., Zhou, J. & Zhang, L. 2012. Structure and solution properties of cyanoethyls cellulose synthesized in LiOH/urea aqueous solution. *Cellulose* 19: 161-169.

Liu, W. 2013. Solutions de cellulose et matériaux hybrides/composites à base de liquides ioniques et solvants alcalins. Thesis. Ecole Nationale Supérieure des Mines de Paris (Unpublished). pp. 4-35.

Luo, X. & Zhang, L. 2013. New solvents and functional materials prepared from cellulose solutions in alkali/urea aqueous system. *Food Research International* 52: 387-400.

Moon, R.J., Martini, A., Nairn, J., Simonsen, J. & Youngblood, J. 2011. Cellulose nanomaterials review: Structure, properties and nanocomposites. *Chem. Soc. Rev*. 40: 3941-3994.

Nazir, M.S., Wahjoedi, B.A., Yussof, A.W. & Abdullah, M.A. 2013. Eco-friendly extraction and characterization of cellulose from oil palm empty fruit bunches. *Bioresources* 8(2): 2161-2172.

Nurdiawati, A., Novianti, S., Zaini, I.N., Nakhshinieva, B., Sumida, H., Takahashi, F. & Yoshikawa, K. 2015. Evaluation of hydrothermal treatment of empty fruit bunch for solid fuel and liquid organic fertilizer co-production. International Conference on Alternative Energy in Developing Countries and Emerging Economies. *Energy Procedia*. 79: 226-232.

Olsson, C. & Westman, G. 2013. Direct dissolution of cellulose: Background, means and applications. *Cellulose - Fundamental Aspect* 6: 143-178.

Rowell, R.M. & Young, R.A. 1978. *Modified Cellulosics*. New York: Academic Press. American Chemical Society. Cellulose, Paper and Textile Division. pp. 10-51.

Saba, Paridah, M.T., Abdan, K. & Ibrahim, N.A. 2016. Dynamic mechanical properties of oil palm nano filler/kenaf/ epoxy hybrid nanocomposites. *Construction and Building Materials* 124: 133-138.

Sajab, M.S., Chia, C.H., Zakaria, S., Jani, S.M., Ayob, M.K., Chee, K.L., Khiew, P.S. & Chin, W.S. 2011. Citric acid modified kenaf core fibers for removal of methylene blue from aqueous solution. *Bioresource Technology* 102(15): 7237-7243.

Siqueira, G., Bras, J. & Dufresne, A. 2010. Luffa cylindrica as a lignocellulosic source of fiber, microfibrillated cellulose and cellulose nanocrystal. *BioResources* 5(2): 727-740.

Strunk, P. 2012. Characterization of cellulose pulps and the influence of their properties on the process and production of viscose and cellulose ethers. PhD Thesis. Department of Chemistry Umea University, Sweden (Unpublished).

Wang, Y. & Deng, Y. 2009. The kinetics of cellulose dissolution in sodium hydroxide solution at low temperatures. *Biotechnology and Bioengineering*.102: 1398-1405.

Xiao, B., Sun, X.F. & Sun, R.C. 2001. Chemical, structural and thermal characterization of alkali-soluble lignins and hemicelluloses and cellulose from maize stems and rice straw. *Polymer Degradation and Stability* 74: 307-319.

Zhang, S., Li, F-X., Yu, J-Y. & Hsieh, Y-L. 2010. Dissolution behaviour and solubility of cellulode in NaOH complex solution. *Carbohydrate Polymers* 81: 668-674.

Zhou, J., Zhang, L. & Cai, J. 2004. Behaviour of cellulose in NaOH/urea aqueous solution characterized by light scattering and viscometry. *Journal of Polymer Science: Part A: Polymer Science* 42: 5911-5920.

Zhou, J. & Zhang, L. 2000. Solubility of cellulose in NaOH/ urea aqueous solution. *Polymer Journal* 32(10): 866-870.

Zhou, J. & Li, J. 2014. Excellent chemical and material cellulose from tunicates: Diversity in cellulose production yield and chemical and morphological structures from different tunicate species. *Cellulose* 21: 3427-3441.

Khairunnisa Waznah Baharin, Sarani Zakaria* Hatika Kaco, Sinyee Gan & Sharifah Nurul Ain Syed Hashim
Bioresources & Biorefinery Laboratory
Faculty of Science & Technology
Universiti Kebangsaan Malaysia
43600 UKM Bangi, Selangor Darul Ehsan
Malaysia

Amanda V. Ellis
School of Chemical Engineering
University of Melbourne
Melbourne, Victoria
Australia

Noraini Talip
Microtechnique and Plant Anatomy Research Team
Faculty of Science & Technology
Universiti Kebangsaan Malaysia
43600 UKM Bangi, Selangor Darul Ehsan
Malaysia

Farrah Diyana Zailan
School of Applied Physics
Faculty of Science & Technology
Universiti Kebangsaan Malaysia
43600 UKM Bangi, Selangor Darul Ehsan
Malaysia

*Corresponding author; email: szakaria@ukm.edu.my

Received: 5 December 2016
Accepted: 31 July 2017